

Supporting Information

Lignin fate and characterization during ionic liquid biomass pretreatment for renewable chemicals and fuels production

Noppadon Sathitsuksanoh¹, Kevin M. Holtman², Daniel J. Yelle³, Trevor Morgan⁴, Vitalie Stavila⁵, Jeffrey Pelton⁶, John Ralph^{7,8}, Harvey Blanch^{1,9}, Blake A. Simmons^{1,5}, Anthe George^{1,5}
*

¹Joint BioEnergy Institute, 5885 Hollis St., Emeryville, CA 94608, USA

²U.S. Department of Agriculture, Agricultural Research Services, Western Regional Research Center, Bioproduct Chemistry and Engineering Research, Albany, CA 94710, USA

³U.S. Forest Service, Forest Products Laboratory, Madison, WI USA

⁴Hawaii Natural Energy Institute, University of Hawaii, USA

⁵Sandia National Laboratory, Livermore, CA, USA

⁶Physical Biosciences Division, Lawrence Berkeley National Laboratory, 1 Cyclotron Rd., Berkeley, CA 94720, USA

⁷Department of Biochemistry, 2113 Wisconsin Energy Institute, University of Wisconsin, Madison, WI 53706, USA

⁸Great Lake Bioenergy Research Center, 1550 Linden Dr., Madison, WI 53706, USA

⁹Department of Chemical and Biomolecular Engineering, University of California, Berkeley, CA 94720-1462, USA

*Correspondence should be addressed to: ageorge@lbl.gov

Changes in degree of crystallinity during pretreatments

XRD spectra of untreated and pretreated samples were shown in **Figure S2**. Untreated biomass samples show three singlets of (101), (002) and (040), corresponding to cellulose I polymorph. High crystallinity indices (CrIs) of 72.5%, 59.3%, and 64.7% were observed for untreated wheat straw, Miscanthus, and pine, respectively. Spectra of pretreated biomass samples at 120 °C revealed a significant reduction in degree of crystallinity and their CrIs were decreased by ~2-fold compared to those of untreated biomass. A further increase in pretreatment temperature from 120 to 160 °C caused CrIs to decrease further for wheat straw and Miscanthus, indicating that at pretreated biomass at 160 °C became less crystalline. CrIs of pretreated pine, however, at 120 °C and 160 °C are comparable, implying that higher pretreatment temperatures

and/or longer pretreatment times are required to decrease degree of crystallinity of pine. CrIs were found to be inversely proportional to enzymatic glucan digestibility (**Fig. S2D**). These results suggested that enhanced enzymatic glucan release after IL pretreatment was partly due to a decrease in CrI and lignin removal. It should be noted that these correlations between lignin extraction efficiency and CrI with enzymatic hydrolysis were drawn according to results from [C₂mim][OAc] in the present study.

Changes in structural polysaccharides after pretreatment

Wheat straw

Aliphatic region of wheat straw cell walls (**Fig. S6A**) exhibit two distinct peaks of 2-*O*-Ac-β-D-Xylp(R) (X'₂) and 3-*O*-Ac-β-D-Xylp(R) (X'₃). A relative ratio of X'₂ : X'₃ of untreated wheat straw was estimated as 0.77. After IL pretreatment at 120 °C, the relative ratio of X'₂ : X'₃ decreased to 0.40. A further increase in pretreatment temperature from 120 to 160 °C caused a further decrease in X'₂ : X'₃ ratio to 0.30. These results implied that deacetylation of hemicelluloses occurred more readily at C₂/H₂ position.

Most correlations in the anomeric region belong to polysaccharide anomers. The untreated wheat straw spectrum (**Fig. S6B**) shows a correlation of cellulose (δ_C/δ_H 103.1/4.39 ppm) and xylan (δ_C/δ_H 101.9/4.38 ppm) with 2-*O*-Ac-β-D-Xylp(R) and 3-*O*-Ac-β-D-Xylp(R) being major acetylated components of hemicelluloses. Reducing ends of (1→4)-β-D-Xylp/Glcp and (1→4)-α-D-Xylp/Glcp were observed and denoted as β-D-Xylp(R)/Glcp(R) and α-D-Xylp(R)/Glcp(R), respectively. 4-*O*-Me-GlcA (4-methoxyl-glucuronic acid) was observed in untreated wheat straw (**Fig. 6SD**). Residue of α-L-arabinofuranosyl (α-L-Araf) units appeared at δ_C/δ_H 108.1/5.3 ppm. After IL pretreatment at 120 and 160 °C, no dramatic changes were

observed in polysaccharides. Interestingly, the α -D-Xylp(R)/Glc p(R) showed a noticeable decrease as pretreatment temperature increased. This might be due to some glycosidic bond cleavage and reduction in degree of polymerization of hemicelluloses after IL pretreatment. After IL pretreatment at 120 °C, a decrease in degree of acetylation from 17.05 to 5.90% was observed, suggesting deacetylation of hemicelluloses, which reduces steric hindrance and enables enzyme accessibility to cellulose (Kong et al. 1992; Samuel et al. 2011), and this is corroborated by enhanced enzymatic glucan hydrolysis (**Fig. S1**). As pretreatment temperature increased from 120 °C to 160 °C, a further decrease in degree of acetylation from 5.90 to 3.75% was observed, confirming that acetyl groups of the xylan can be readily removed by IL pretreatment at higher temperature, resulting in a further reduction in steric hindrance as shown in a greater enhancement of enzymatic glucan digestibility of pretreated wheat straw at 160 °C than that of 120 °C. At 160 °C, a large amount of lignin was solvated during IL pretreatment. As such, the pretreated wheat straw at 160 °C contains less lignin and no aromatic units were observed in aromatic region (**Fig. S6I**).

Miscanthus

The aliphatic region of the 2D HSQC spectrum of untreated Miscanthus (**Fig. S7A**) shows two distinct peaks of X'_2 and X'_3 . A decrease in volume integration of X'_2 and X'_3 and levels of FA indicated pretreated Miscanthus at 120 °C was more susceptible to enzymatic hydrolysis, which corresponds well to the hydrolysis result in **Figure S1**. Similar to wheat straw, an increase in pretreatment temperature to 160 °C resulted in a decrease in degree of acetylation (**Table S4**), resulting in an increase in enzymatic glucan digestibility of pretreated Miscanthus at 160 °C compared to that of 120 °C due to less steric hindrance.

The polysaccharide anomeric correlations of untreated Miscanthus (**Fig. S7B**) were similar to those of untreated wheat straw. No significant changes were observed in the anomeric region of pretreated Miscanthus at 120 and 160 °C. An increase in pretreatment temperature showed a weaker α -D-Xylp(R)/GlcP(R) correlation due to breaking of glycosidic bonds and decreasing degree of polymerization of hemicelluloses. Moreover, at 160 °C, a large amount of lignin was solvated during IL pretreatment. As such, the pretreated Miscanthus at 160 °C contains less lignin and no aromatic units were observed in aromatic region (**Fig. S6I**).

Pine

Different from wheat straw and Miscanthus, pine contains high amounts of galactoglucomannan (**Table S1**) with *O*-acetylated mannan groups in the form of β -mannosyl units at position C₂ and C₃. The anomeric polysaccharide region (**Fig. S8B**) revealed the anomeric from β -D-mannopyranosyl [(1 \rightarrow 4)- β -D-Manp] residues at δ_C/δ_H 100.7/4.63 ppm and reducing ends of α -D-mannopyranosyl [(1 \rightarrow 4)- α -D-Manp] at 94.0/5.05 ppm. The anomeric 2-*O*-Ac- β -D-Manp at δ_C/δ_H 98.9/4.86 ppm and 3-*O*-Ac- β -D-Manp at δ_C/δ_H 99.9/4.78 ppm were observed. Two peaks in the area of δ_C/δ_H 106-109/4.7-5.4 ppm are believed to be α -L-arabinofuranosyl (α -L-Araf) (Kim and Ralph 2010). Pretreated pine at 120 and 160 °C showed an absence of *O*-acetylated galactoglucomannans (2-*O*-Ac- β -D-Manp in the aliphatic region as well as 2-*O*-Ac- β -D-Manp and 3-*O*-Ac- β -D-Manp in anomeric region), which was due to deacetylation from IL pretreatment at 120 and 160 °C. Consequently, pretreated pine at 120 °C and 160 °C yielded enhanced enzymatic hydrolysis. The effect of an increase in pretreatment temperature from 120 °C to 160 °C was not pronounced, as shown in a slight increase in enzymatic glucan digestibility (**Figure S1C**). This result indicates that pine is less susceptible to

enzymatic saccharification and that harsher pretreatment conditions (e.g., longer pretreatment time, higher temperature/pressure) are required to overcome recalcitrance of pine.

Supporting information

Table S1. Compositional analysis of wheat straw, Miscanthus, and pine before and after pretreatment at 120 and 160 °C

Composition (wt.%)	Wheat straw			Miscanthus			Pine		
	Untreated	Pretreated		Untreated	Pretreated		Untreated	Pretreated	
		120 °C	160 °C		120 °C	160 °C		120 °C	160 °C
Solid recovery	100.0±0.7	76.0±1.7	60.4±1.5	100.0±1.1	84.8±1.1	63.1±1.6	100.0±0.8	87.6±1.3	70.9±0.8
Glucan	39.5±0.1	49.0±1.7	58.8±1.1	48.1±0.4	51.6±0.5	62.49±0.02	41.2±2.9	43.1±0.3	47.1±0.3
Xylan	18.8±0.2	21.5±0.6	21.4±0.4	17.9±0.1	20.04±0.04	20.9±0.3	6.4±0.2	6.9±0.1	5.86±0.04
Galactan	-	-	-	-	-	-	2.41±0.04	2.28±0.03	1.82±0.02
Arabinan	-	-	-	-	-	-	1.8±0.1	1.80±0.04	1.7±0.1
Mannan	-	-	-	-	-	-	11.2±0.8	10.8±0.1	9.48±0.01
Lignin	21.6 ± 0.1	18.1±0.3	8.1±0.3	24.6±0.2	18.6±0.2	8.6±0.6	32.2±1.4	31.03±0.1	31.1±0.3
Ash	2.9±0.1	2.5±0.5	4.2±0.3	1.2±0.1	2.04±0.01	1.4±0.4	ND	ND	ND
Others	17.2±0.3	8.9±1.9	7.5±1.3	8.2±0.5	7.7±0.5	6.6±0.8	4.8±3.3	4.1±0.4	2.9±0.4

Table S2. Overall glucose and xylose yields of pretreated biomass hydrolyzed by Ctec 2, after 72hr

Feedstock\ pretreatment condition	120 °C					160 °C				
	Glucose yield (%)		Xylose yield (%)		Lignin extraction (%)	Glucose yield (%)		Xylose yield (%)		Lignin extraction (%)
	Enzymatic	Overall	Enzymatic	Overall		Enzymatic	Overall	Enzymatic	Overall	
Wheat straw	80.0 ± 2.1	81.2 ± 5.8	69.7 ± 1.1	73.7 ± 5.3	36.3 ± 1.9	98.4 ± 1.6	97.6 ± 4.5	97.3 ± 0.6	94.3 ± 4.0	77.4 ± 2.3
Miscanthus	85.4 ± 1.1	86.7 ± 2.5	75.5 ± 0.4	76.7 ± 2.3	35.9 ± 1.6	99.0 ± 1.4	97.4 ± 3.2	98.4 ± 0.5	95.6 ± 3.1	77.9 ± 2.3
Pine	70.6 ± 1.3	73.1 ± 8.7	55.9 ± 0.3	58.4 ± 5.2	15.6 ± 1.2	91.0 ± 2.9	90.8 ± 9.3	87.7 ± 0.1	87.7 ± 4.2	31.5 ± 2.8

Table S3. Assignments of the lignin ^{13}C - ^1H correlation peaks in the 2D HSQC spectra of wheat straw, Miscanthus, and pine

Region	Label	$\delta_{\text{C}}/\delta_{\text{H}}$ (ppm)	Assignment
Aliphatic	A $_{\alpha}$	71.8/4.83	C $_{\alpha}$ -H $_{\alpha}$ in β -O-4' substructures (A)
	A $_{\beta(\text{G})}$	83.4/4.27	C $_{\beta}$ -H $_{\beta}$ in β -O-4' substructures (A) linked to a G unit
	A $_{\beta(\text{S})}$	85.9/4.10	C $_{\beta}$ -H $_{\beta}$ in β -O-4' substructures linked (A) to a S unit
	B $_{\alpha}$	86.8/5.43	C $_{\alpha}$ -H $_{\alpha}$ in β -5 phenylcoumaran substructures (B)
	B $_{\beta}$	53.1/3.43	C $_{\beta}$ -H $_{\beta}$ in β -5 phenylcoumaran substructures (B)
	C $_{\alpha}$	84.8/4.65	C $_{\alpha}$ -H $_{\alpha}$ in β - β' resinol substructures (C)
	C $_{\beta}$	53.5/3.05	C $_{\beta}$ -H $_{\beta}$ in β - β' resinol substructures (C)
	C $_{\gamma}$	71.0/4.17	C $_{\gamma}$ -H $_{\gamma}$ in β - β' resinol substructures (C) only seen in WS and MC
	D $_{\alpha}$	83.3/4.81	C $_{\alpha}$ -H $_{\alpha}$ in dibenzodioxocin substructures (D) only seen in WS and MC
	E $_{\gamma}$	61.3/4.08	C $_{\gamma}$ -H $_{\gamma}$ in cinnamyl alcohol end-groups (E) overlaps with carbohydrate signals
	MeO (-OCH $_3$)	55.6/3.73	C-H in methoxyls
Aromatic	H $_{2,6}$	127.8/7.22	C $_{2,6}$ -H $_{2,6}$ in <i>p</i> -hydroxyphenyl units (H) in WS and MC
	G $_2$	110.9/6.99	C $_2$ -H $_2$ in guaiacyl units (G)
	G $_5$ /G $_6$	114.9/6.72 and 6.94	C $_5$ -H $_5$ and C $_6$ -H $_6$ in guaiacyl units (G)
	G $_5$	118.7/6.77	C $_5$ -H $_5$ in guaiacyl units (G)
	S $_{2,6}$	103.8/6.69	C $_2$ -H $_2$ and C $_6$ -H $_6$ in etherified syringyl units (S)
	<i>p</i> CA $_{2,6}$	130.1/7.45	C $_2$ -H $_2$ and C $_6$ -H $_6$ in <i>p</i> -coumarate (pCA) in WS and MC
	FA $_2$	110.9/7.33	C $_2$ -H $_2$ in ferulate (FA) in WS and MC
T $_{2,6}$	103.3/7.19	C $_2$ -H $_2$ in triclin (T) in WS	

Table S4. Changes in C $_2$ - and C $_3$ -acetylated hemicelluloses of different biomass during pretreatment

Feedstock	Wheat straw			Miscanthus			Pine		
	Untreated	Pretreated at 120 °C	Pretreated at 160 °C	Untreated	Pretreated at 120 °C	Pretreated at 160 °C	Untreated	Pretreated at 120 °C	Pretreated at 160 °C
Degree of acetylation	17.05	5.90	3.75	39.87	5.90	3.88	77.36	15.35	11.54
X $_2$: X $_3$	0.77:1.00	0.40:1.00	0.30:1.00	0.67:1.00	0.45:1.00	0.30:1.00	ND	ND	ND

Supporting information

Figure S1. Enzymatic glucan digestibility profiles of pretreated wheat straw (A), Miscanthus (B), and pine (C).

Figure S2. XRD spectra of pretreated wheat straw (A), Miscanthus (B), and pine (C). Changes in the crystallinity index of cellulose were depicted as a function of enzymatic glucan digestibility (D), as hemicelluloses and lignin hardly contribute to degree of crystallinity.

Figure S3. Complete mass balance diagram of IL pretreatment, followed by enzymatic hydrolysis of wheat straw, Miscanthus, and pine at 120 °C.

Figure S4. Complete mass balance diagram of IL pretreatment, followed by enzymatic hydrolysis of wheat straw, Miscanthus, and pine at 160 °C.

Figure S5. Area-normalized SEC chromatograms of L₁ from wheat straw, Miscanthus, and pine by UV-A₃₀₀. L₁ denotes lignin from untreated biomass.

Figure S6. 2D HSQC NMR spectra of nonderivatized wheat straw cell walls before and after IL pretreatment at 120 and 160 °C ; aliphatic (A, D, and G), anomeric (B, E, and H) and aromatic (C, F, and I) regions of the HSQC spectrum. All contours are color-coded to match their respective structures in **Figure S9**. See **Table S3** for structural characteristics from integration of ¹³C-¹H correlation peaks in the HSQC.

Figure S7. 2D HSQC NMR spectra of nonderivatized Miscanthus cell walls before and after IL pretreatment at 120 and 160 °C ; aliphatic (A, D, and G), anomeric (B, E, and H) and aromatic (C, F, and I) regions of the HSQC spectrum. All contours are color-coded to match their respective structures in **Figure S9**. See **Table S3** for structural characteristics from integration of ¹³C-¹H correlation peaks in the HSQC.

Figure S8. 2D HSQC NMR spectra of nonderivatized pine cell walls before and after IL pretreatment at 120 and 160 °C ; aliphatic (A, D, and G), anomeric (B, E, and H) and aromatic (C, F, and I) regions of the HSQC spectrum. All contours are color-coded to match their respective structures in **Figure S9**. See **Table S3** for structural characteristics from integration of ¹³C-¹H correlation peaks in the HSQC.

Figure S9. Main structures present in the lignins of wheat straw, Miscanthus, and pine: (A) β -O-4 aryl ethers; (B) phenylcoumarans; (C) resinols; (D) dibenzodioxocins; (E) cinnamyl alcohol end-groups; (*pCA*) *p*-coumarates; (FA) ferulates; (G) guaiacyl units; (S) syringyl units. Peak assignments are shown in **Table S3**.

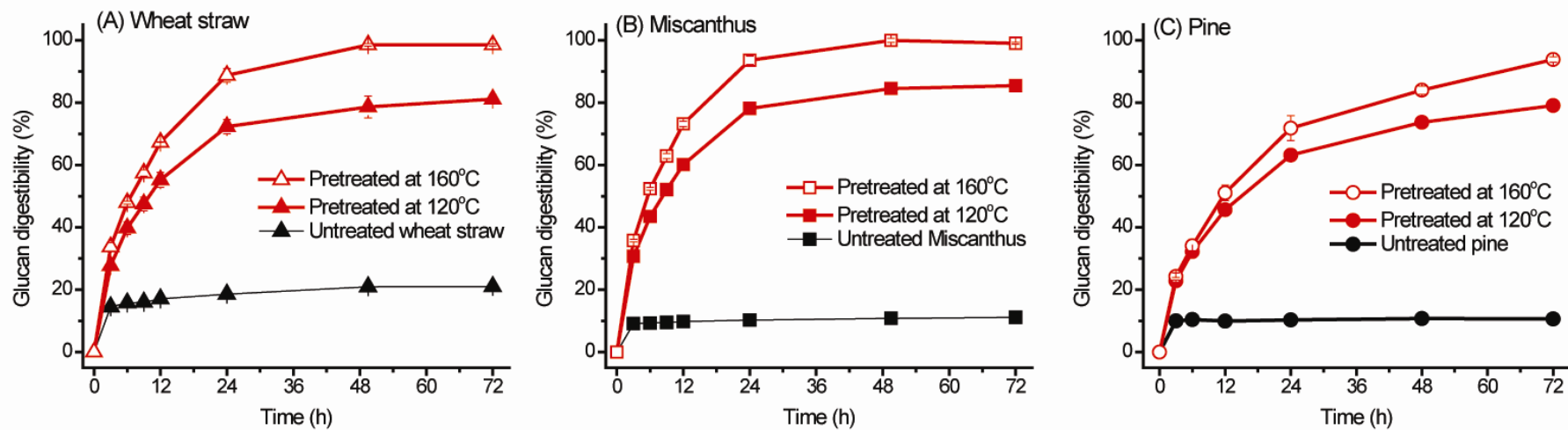


Fig. S1

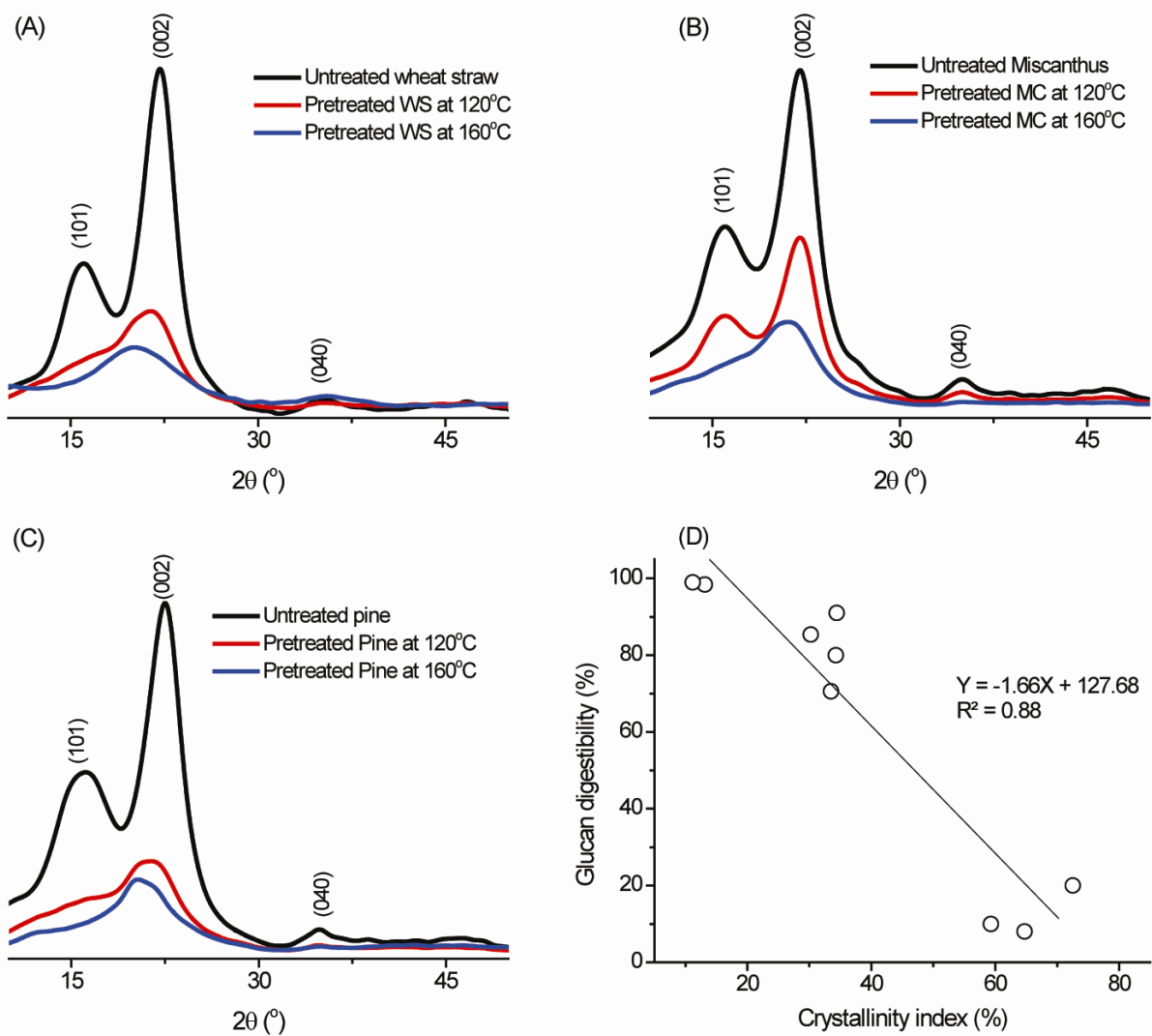


Fig. S2

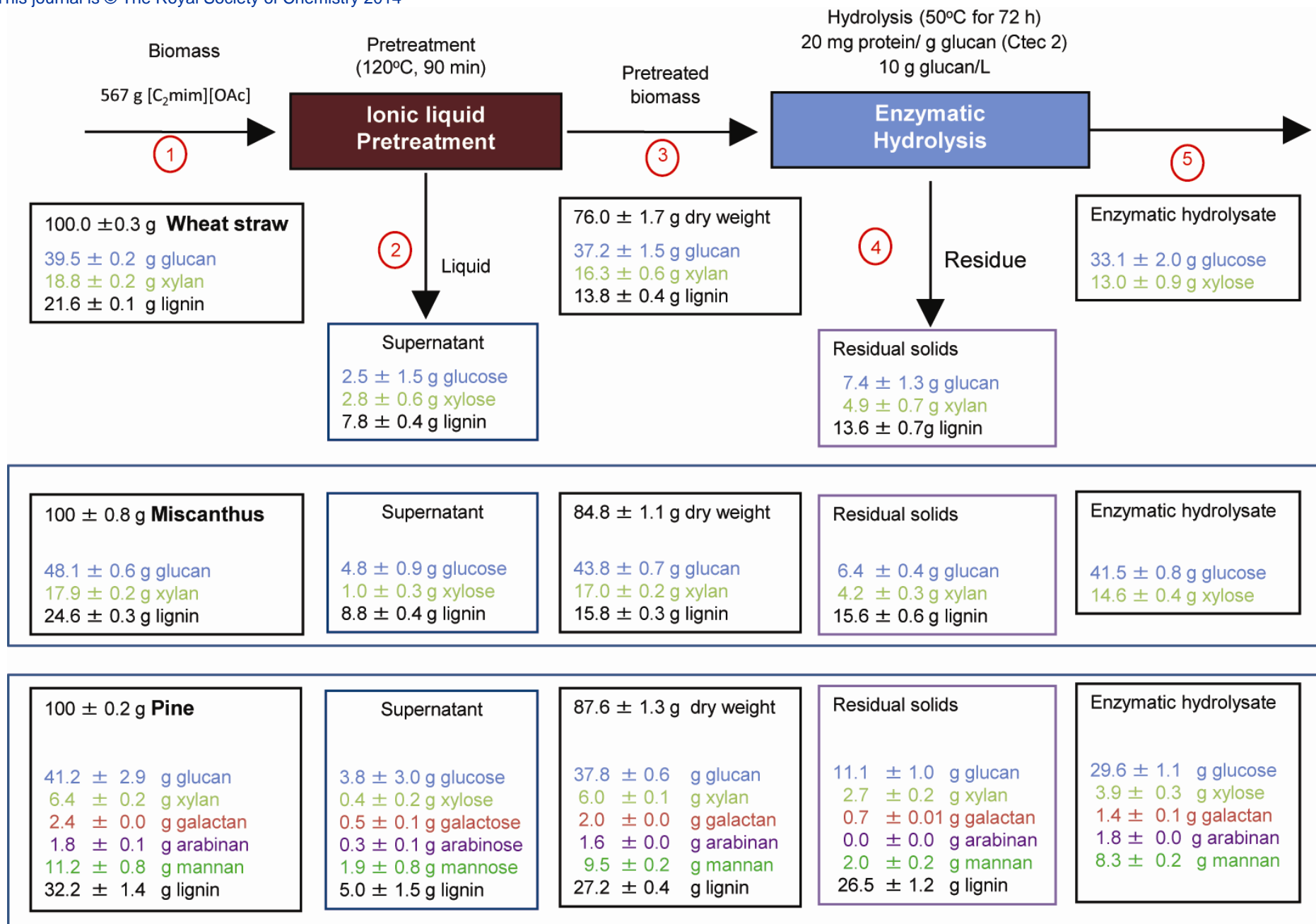


Fig. S3

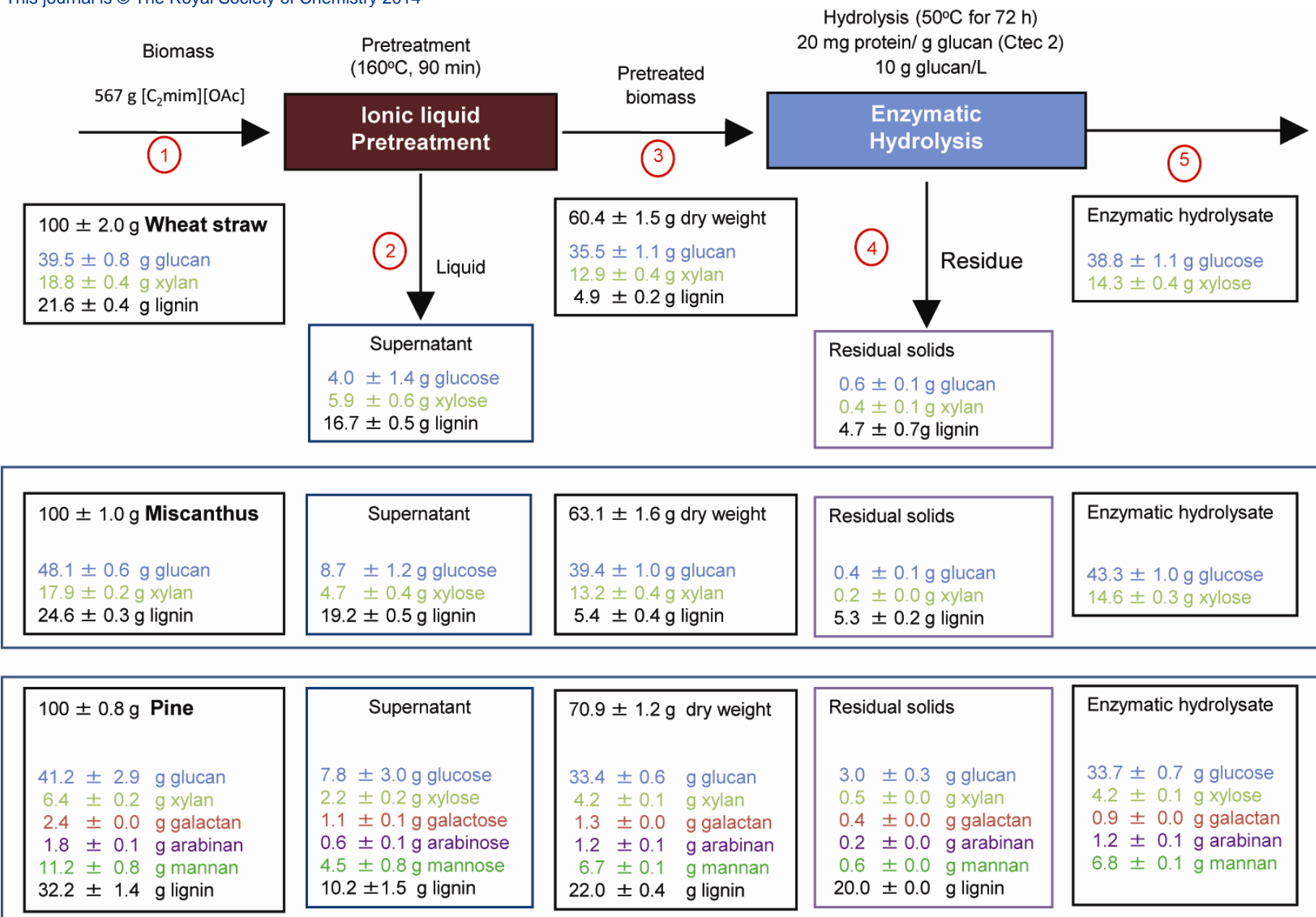


Fig. S4

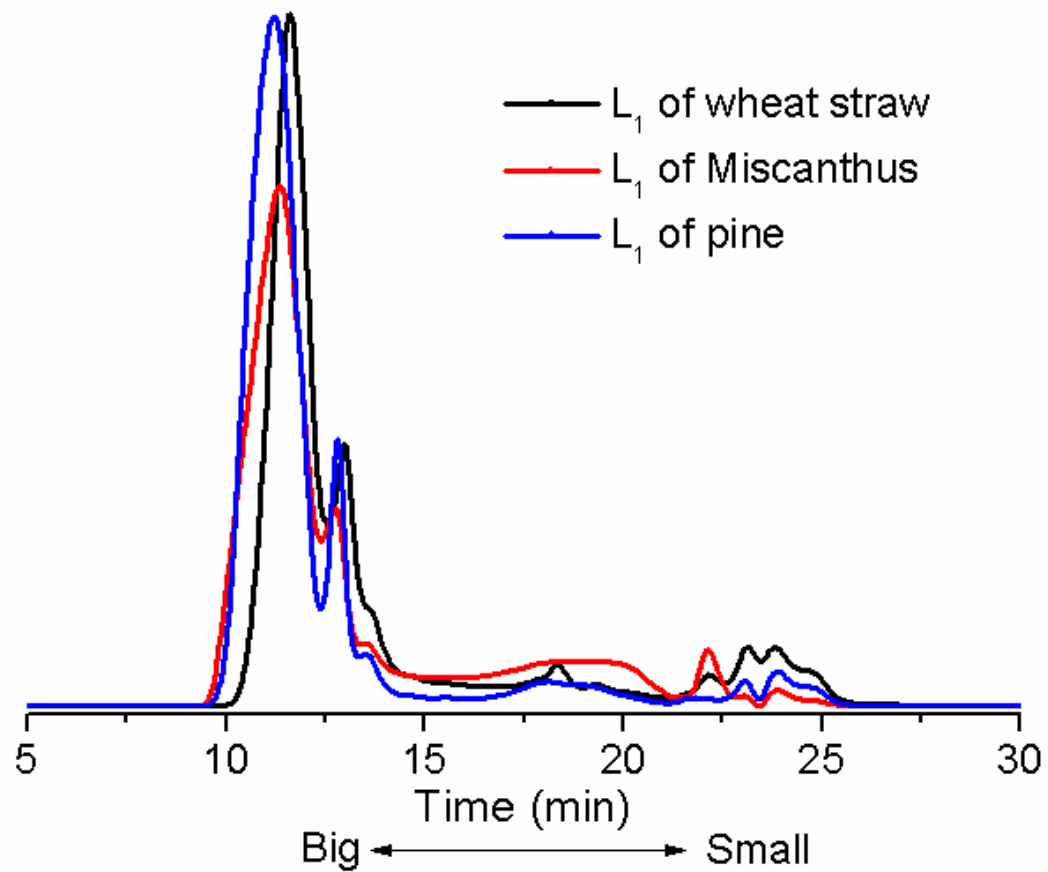


Fig. S5

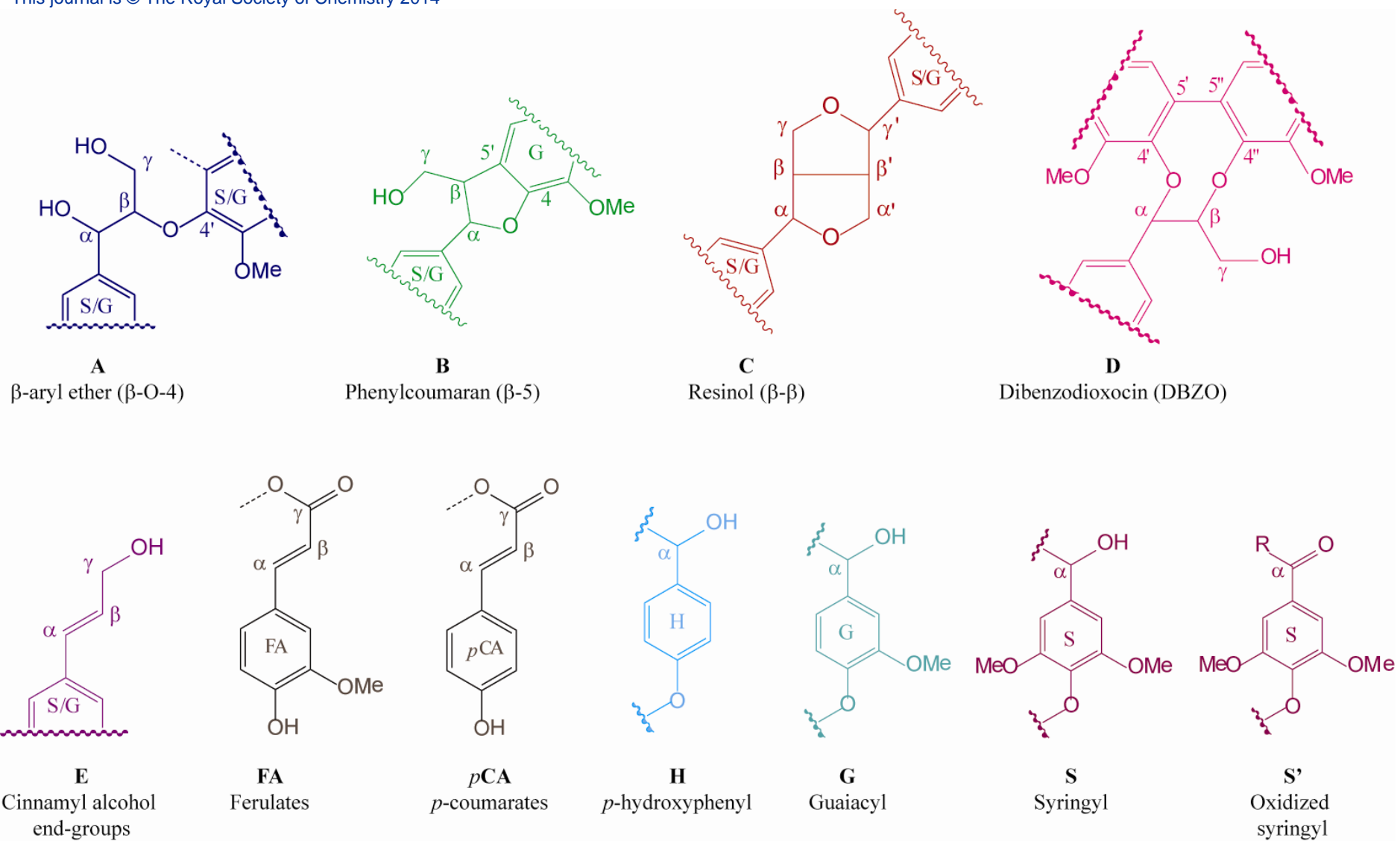


Fig. S9

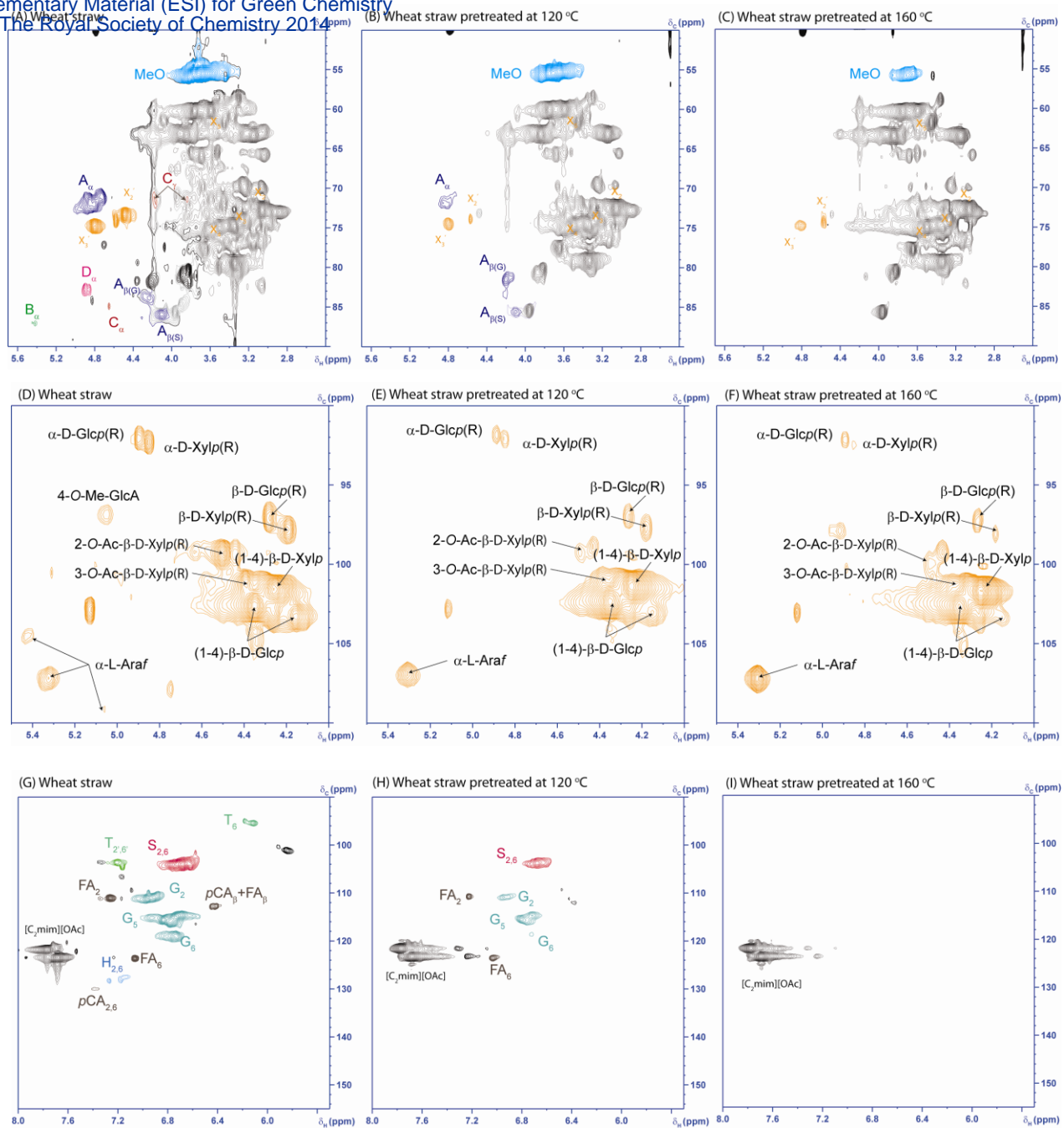


Fig. S6

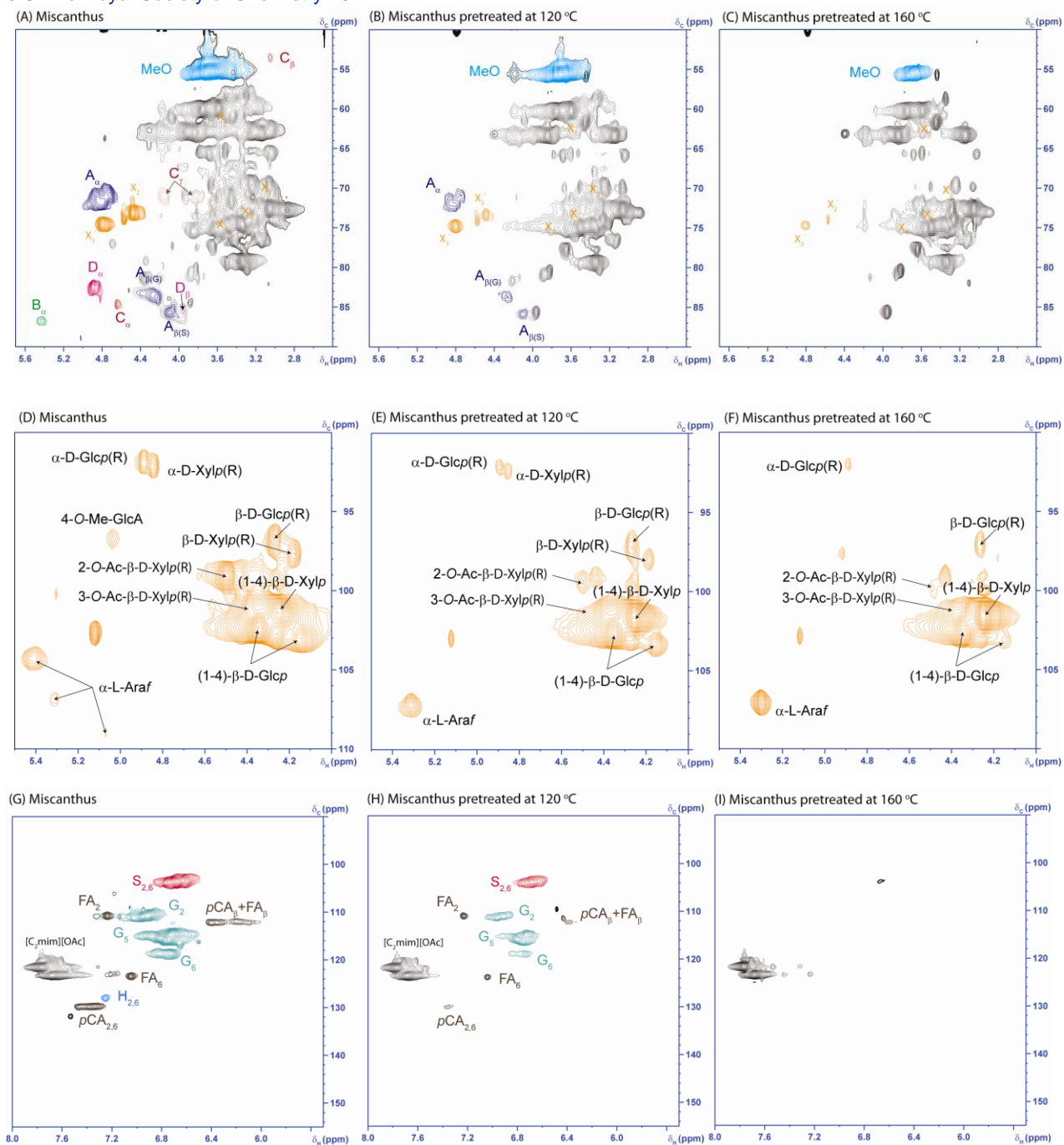


Fig. S7

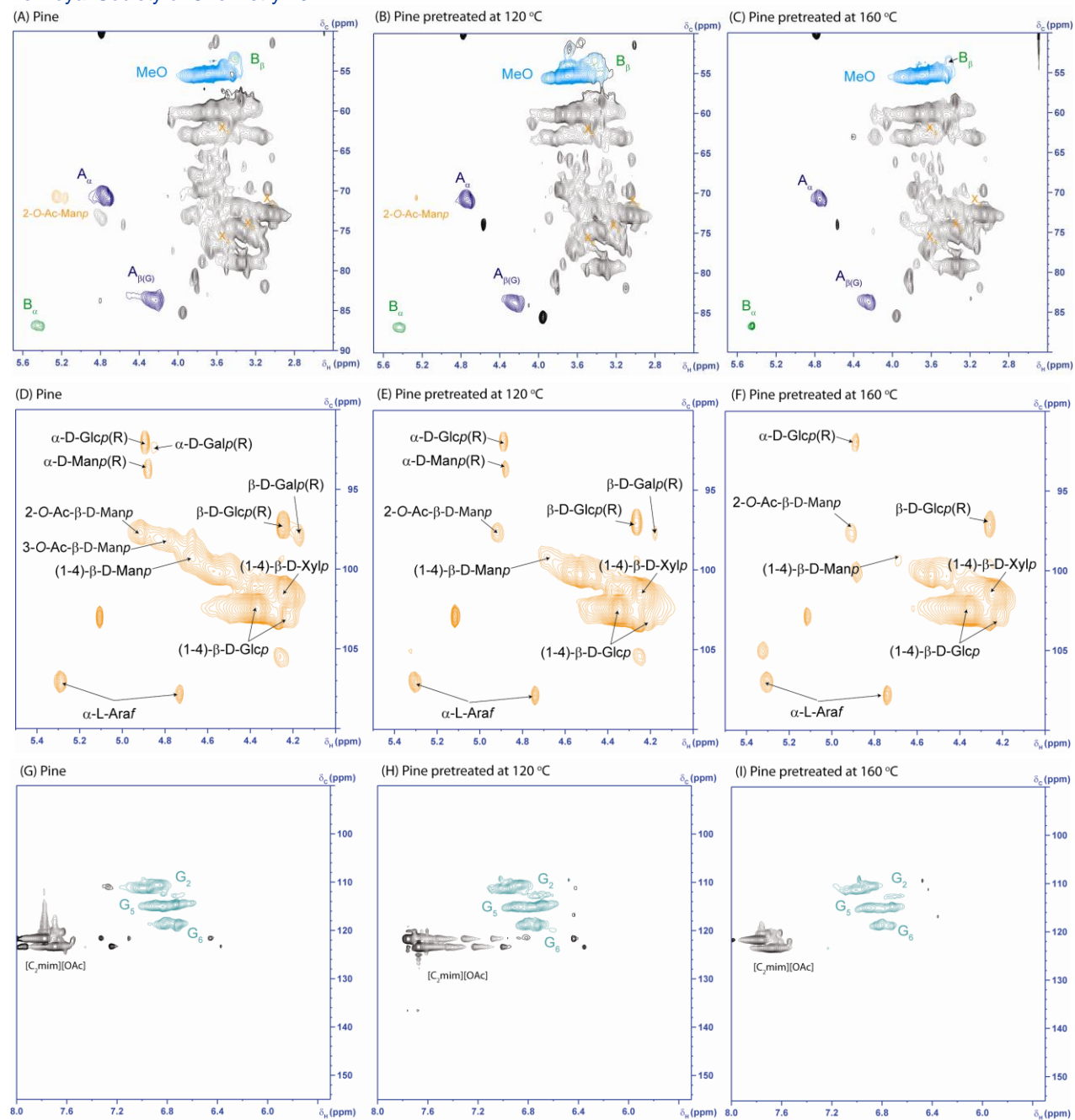


Fig. S8